

ARTICLE

Population Pharmacokinetic/Pharmacodynamic Modeling of Methylprednisolone in Neonates Undergoing Cardiopulmonary Bypass

Christoph P. Hornik^{1,*}, Daniel Gonzalez², Julie Dumond², Huali Wu¹, Eric M. Graham³, Kevin D. Hill¹ and Michael Cohen-Wolkowicz¹

Methylprednisolone is used in neonates to modulate cardiopulmonary bypass (CPB)–induced inflammation, but optimal dosing and exposure are unknown. We used plasma methylprednisolone and interleukin (IL)–6 and IL–10 concentrations from neonates enrolled in a randomized trial comparing one vs. two doses of methylprednisolone to develop indirect response population pharmacokinetic/pharmacodynamic models characterizing the exposure–response relationships. We applied the models to simulate methylprednisolone dosages resulting in the desired IL–6 and –10 exposures, known mediators of CPB-induced inflammation. A total of 64 neonates (median weight 3.2 kg, range 2.2–4.3) contributed 290 plasma methylprednisolone concentrations (range 1.07–12,700 ng/mL) and IL–6 (0–681 pg/mL) and IL–10 (0.1–1125 pg/mL). Methylprednisolone plasma exposure following a single 10 mg/kg intravenous dose inhibited IL–6 and stimulated IL–10 production when compared with placebo. Higher (30 mg/kg) or more frequent (twice) dosing did not confer additional benefit. Clinical efficacy studies are needed to evaluate the effect of optimized dosing on outcomes.

Study Highlights

WHAT IS THE CURRENT KNOWLEDGE ON THE TOPIC?

☑ Methylprednisolone is administered to > 60% of neonates undergoing surgery on cardiopulmonary bypass despite the lack of population-specific dosing, efficacy, and safety data.

WHAT QUESTION DID THIS STUDY ADDRESS?

☑ We developed two separate population pharmacokinetic/pharmacodynamic (PK/PD) models of methylprednisolone to help inform optimal dosing for a future study.

WHAT DOES THIS STUDY ADD TO OUR KNOWLEDGE?

☑ Methylprednisolone plasma exposure following a single 10 mg/kg intravenous dose inhibited

interleukin (IL)–6 and stimulated IL–10 production when compared with placebo. Higher (30 mg/kg) or more frequent (twice) dosing did not confer additional benefit.

HOW MIGHT THIS CHANGE DRUG DISCOVERY, DEVELOPMENT, AND/OR THERAPEUTICS?

☑ We developed the first population PK/PD models for neonates undergoing cardiopulmonary bypass. Our models may be leveraged to simulate methylprednisolone dosing regimens and help inform the design of PK/PD models for other drugs used in this population.

Congenital heart diseases (CHDs) affect ~ 40,000 live births annually in the United States.^{1,2} Severe CHDs need surgery in the neonatal period, which requires cardiopulmonary bypass (CPB) to perform cardiac and pulmonary functions during the operation.³ CPB induces inflammation modulated by cytokines, including proinflammatory interleukin (IL)–6 and anti-inflammatory IL–10, which may lead to postoperative complications and mortality.^{4–7} The suppression of IL-mediated inflammation may be achieved with anti-inflammatory drugs such as methylprednisolone and could improve outcomes, although clinical benefit has not been definitively demonstrated in neonates.

Methylprednisolone is administered to > 60% of neonates on CPB despite a lack of population-specific dosing, efficacy, and safety data.⁸ Intravenous (i.v.) methylprednisolone is given as phosphate or succinate ester prodrugs that are rapidly converted to active drug. Methylprednisolone is lipophilic, moderately bound to plasma albumin, and exhibits linear elimination via oxidation and conjugation in the liver.⁹ Methylprednisolone sodium succinate i.v. is a high extraction rate drug at lower doses with reported clearance (CL) in adults of 82–97 L/hour.^{10,11} CPB may alter methylprednisolone disposition through multiple mechanisms.^{12–15} In adults undergoing CPB, CL was reduced twofold when compared with healthy controls, likely because of impaired

¹Duke Clinical Research Institute, Duke University School of Medicine, Durham, North Carolina, USA; ²Division of Pharmacotherapy and Experimental Therapeutics, University of North Carolina Eshelman School of Pharmacy, The University of North Carolina at Chapel Hill, Chapel Hill, North Carolina, USA; ³Department of Pediatrics, Medical University of South Carolina, Charleston, South Carolina, USA. *Correspondence: Christoph P. Hornik (Christoph.hornik@duke.edu)

Received: May 23, 2019; accepted: August 21, 2019. doi:10.1002/psp4.12470

hepatic blood flow. Methylprednisolone pharmacokinetics (PK) have never been studied in neonates undergoing CPB, and the extrapolation of adult data is inadequate given the developmental and disease-specific changes in drug disposition as well as differences in CPB execution.

Methylprednisolone exposure targets associated with the reduction of CPB-mediated inflammation are unknown. Because of this uncertainty, prior trials studying the relationship between methylprednisolone dosing and clinical end points yielded conflicting results.^{16–20} IL-6 and IL-10 are elevated during CPB in neonates, and the degree of elevation can be modulated by methylprednisolone.¹⁷ Therefore, IL-6 and IL-10 may represent biomarker surrogates for methylprednisolone efficacy. Indirect response PK/pharmacodynamic (PD) models have best characterized methylprednisolone's effects in adults.²¹

The goal of our analyses is to address both knowledge gaps in the PK and PK/PD relationships of methylprednisolone in neonates undergoing CPB. We developed separate population PK/PD (popPK/PD) models for IL-6 and IL-10, leveraging the models to conduct methylprednisolone dosing simulations achieving optimal suppression of IL-6 and induction of IL-10.

METHODS

Study design

Plasma samples and clinical data for this analysis were collected in a prospective, randomized study of methylprednisolone sodium succinate administered as one or two doses of 30 mg/kg via i.v. infusion over 1 hour to neonates \leq 30 days of age prior to CPB (ClinicalTrials.gov, NCT00934843).^{16,22} Per protocol, subjects in the two-dose arm received methylprednisolone approximately 10 hours prior to CPB and at CPB induction into the pump. Subjects in the one-dose arm received methylprednisolone at CPB induction into the pump. Blood samples were collected: Prior to first dose of methylprednisolone; ~8 hours after first dose (for the two-dose group); prior to CPB initiation and second dose; and 0, 4, 12, and 24 hours after the end of CPB. Samples were stored at -80°C without intermittent thawing/refreezing for up to 7 years. PK profiles based on these samples have not been previously published.

Bioanalysis

Plasma methylprednisolone concentrations were quantified using high-performance liquid chromatography tandem mass spectrometry assay. The linear concentration range of methylprednisolone was 20–10,000 mcg/mL, with a lower limit of quantification of 1 ng/mL. Interrun and intrarun precision and accuracy were within the standards established by the US Food and Drug Administration ($< 15\%$ coefficient of variation and bias). Concentrations of IL-6 and IL-10 in plasma were determined via commercially available multiplex suspension array assays (R&D Systems, Minneapolis, MN).¹⁶

PopPK/PD model development

Sequential popPK/PD models were developed using the nonlinear mixed-effect modeling software NONMEM (version 7.2; Icon Development Solutions, Ellicott City, MD) with first-order conditional estimate method with interaction for all runs.

To develop the popPK component of the popPK/PD model, one-compartment and two-compartment models as well as proportional, additive, and combined residual error models were explored. Because methylprednisolone was administered to subjects as methylprednisolone sodium succinate, the formation of methylprednisolone from methylprednisolone sodium succinate was tested for inclusion in the model as a linear kinetic process as previously described.²³ Weight was included *a priori* as a covariate for all structural model parameters (CL, central volume of distribution, peripheral volume of distribution, intercompartmental clearance (Q)), centered to 3.2 kg median weight in our study cohort, and allometrically scaled. We tested both fixed (0.75 and 1 for all CL and V parameters, respectively) and estimated allometric coefficients.

Upon development of the popPK model, individual PK parameter estimates were fixed in the PD analysis to predict methylprednisolone plasma concentrations at the time of IL-6 and IL-10 assessment and fit the population PD component of the popPK/PD model. Based on visual inspection of observed PK/PD data and a previously published PD model for methylprednisolone, direct and indirect effect models were tested.²¹ Because of the known induction of both IL-6 and IL-10 production by CPB, we tested different methods to include CPB onset in the model, including CPB effect as a covariate on the maximum drug effect (e.g., maximum fold change in IL-10 production (S_{max}), maximum fold change in IL-6 production (I_{max})) and CPB as a separate effect on the formation rate (R_{in}) of IL-6 and IL-10 in parallel with drug effect, with or without complete or partial interactions between CPB and drug effects. Based on the delayed change in observed IL-6 and IL-10 concentrations after CPB start, a delay of 0.5 hour in the onset of CPB effect was implemented. Because the observed data showed a protracted decline in IL-6 concentrations after CPB, a half-life for the withdrawal of CPB effect was estimated for IL-6.

The change in IL-6 concentration over time in a model without, with complete, and with partial interaction between CPB effect and drug effect were described using Eqs. 1, 2, and 3, respectively. The relationship between IL-6 formation and decline is shown in Eq. 4, and the parameterization of drug and CPB effect are shown in Eqs. 5 and 6.

$$\frac{d\text{IL-6}}{dt} = R_{\text{in}} \times (1 + \text{CPBFX} - \text{DFX}) - R_{\text{out}} \times \text{IL-6} \quad (1)$$

$$\frac{d\text{IL-6}}{dt} = R_{\text{in}} \times (1 + \text{CPBFX}) \times (1 - \text{DFX}) - R_{\text{out}} \times \text{IL-6} \quad (2)$$

$$\begin{aligned} \frac{d\text{IL-6}}{dt} = R_{\text{in}} * \left[\left(1 + \text{CPBFX} \times \left(1 - \frac{\text{PER}}{100} \right) \right) \times (1 - \text{DFX}) \times \text{STRT} \right. \\ \left. + \text{CPBFX} \times \frac{\text{PER}}{100} + (1 - \text{STRT}) \times (1 - \text{DFX}) \right] - R_{\text{out}} \times \text{IL-6} \end{aligned} \quad (3)$$

$$R_{\text{in}} = R_{\text{out}} \times \text{IL-6}_{\text{base}} \quad (4)$$

$$\text{DFX} = \frac{I_{\text{max}} \times C_p^{\text{HILL}}}{\text{IC}_{50}^{\text{HILL}} + C_p^{\text{HILL}}} \quad (5)$$

$$\text{CPBFX} = \text{CPBE} \times \left(1 \times \text{ONCPB} \times \text{CPBES} \right. \\ \left. + (1 - \text{ENDT}) \times \text{EXP} \left(-0.693 \times \frac{\text{TACPB}}{\text{CPBH}} \right) \right) \quad (6)$$

where R_{in} is the zero-order rate for production of IL-6, R_{out} is the first-order rate for decline of IL-6. $IL-6_{base}$ is the model-predicted IL-6 plasma concentration prior to the first dose. I_{max} is the maximum fold change in the production of IL-6 as a response to drug exposure. IC_{50} is the methylprednisolone concentration that produces 50% of maximum attainable inhibition. HILL is the Hill coefficient. C_p is the predicted plasma concentration of methylprednisolone. CPBE is the fold change in IL-6 as a response to CPB procedure. CPBV is a function describing the temporal effects of CPB. PER is the percent interaction between CPB and drug effects. ONCPB is a dummy indicator variable that takes the value 0 for no CPB and 1 during CPB. CPBES, used to represent the delay in CPB effect onset, is 0 for the first 30 minutes after start of CPB and 1 thereafter. STRT is 0 prior to start of CPB and 1 thereafter. ENDT is 0 post-CPB stop and 1 prior to CPB stop. TACPB is the time after the end of CPB. CPBH is the half-life of CPB effect. DFX and CPBFX are equations illustrating the drug and CPB effects, respectively. Changes in IL-10 plasma concentrations over time were characterized using equations similar to those for IL-6 except a stimulatory E_{max} model (S_{max}) accounting for the stimulation effect of methylprednisolone on R_{in} for IL-10. Clinical covariates were analyzed for inclusion in the PK and PD components of the model (see **Supplementary Methods** for details).

PopPK/PD model evaluation

Standard diagnostic methods for assessment of the popPK/PD model performance were applied: Successful minimization, diagnostic plots, plausibility and precision of parameter estimates, objective function value (OFV), and shrinkage value. Nonparametric bootstrapping (500 replicates) was performed to evaluate precision of the final popPK/PD model parameter estimates and to generate 95% confidence intervals (CIs).

Prediction-corrected visual predictive checks and standardized visual predictive check (SVPC) were performed for the final popPK and popPK/PD models by generating 1,000 Monte Carlo simulation replicates per time point.²⁴ Simulated results were compared with those observed in the study, including calculating and plotting the percentile of each observed concentration in relation to its 1,000 simulated observations derived from the final model for the SVPC.²⁵ The dosing and covariate values used to generate the predictions were the same as those used in the study population. The number of observed concentrations outside of the 90% prediction interval for each time point was quantified.

Dosing simulation

The final popPK/PD models were used to simulate IL-6 and IL-10 concentration time profiles in virtual subjects mimicking clinical scenarios. Using PK-Sim (Open Systems Pharmacology Suite, open-systems-pharmacology.com),

a virtual population of 1,000 term infants (gestational age 40 weeks) with 50% female and 85% white Americans (15% black Americans) were generated for the following equally distributed age groups: Postnatal age (PNA) of 0–≤ 7 days, > 7–14 days, > 14–28 days, and 0–28 days. For IL-6 simulations, Risk Adjustment for Congenital Heart Surgery (RACHS-1) scores < 4 or ≥ 4 were randomly assigned in equal distribution regardless of PNA. A RACHS-1 score cutoff ≥ 4 was selected because it was previously associated with fivefold or greater odds of mortality when compared with RACHS-1 scores < 4²⁶ and because subjects with scores ≥ 4 had mostly positive deviations of individual CL estimates from the population mean compared with scores < 4, which had mostly negative deviations. Within each RACHS-1 group, CPB durations of 1–< 2 hours, 2–< 3 hours, and 3–4 hours were randomly assigned. For IL-10 simulations, three different time lengths of CPB (1–< 2 hours, 2–< 3 hours, and 3–4 hours) were assigned to each of three distinct age groups: PNA 0–≤7 days, 8–14 days, and > 14–28 days. For each scenario, two dose levels of methylprednisolone (10 and 30 mg/kg) and a scenario without methylprednisolone were assigned. At each dose, two dosing frequencies were tested: One dose at CPB initiation and one dose at CPB initiation plus an additional dose 8 hours prior. Simulated concentration time curves of IL-6 and IL-10 were plotted and visually compared across dosing simulations. Area under the concentration-time curve from time 0–24 hours after CPB start (AUC_{0-24}) was calculated in NONMEM for IL-6 and IL-10 using simulated concentrations for each scenario and the following equation (Eq. 7):

$$AUC_{0-24} = \int_{t_1}^{t_1+24} C dt \quad (7)$$

where C is the concentration of IL-6 or IL-10, t_1 is time of the CPB start relative to time of the first dose, and t is time after the first dose. Summary statistics including mean, standard deviation, median, minimum, maximum, and 95% CI were calculated for AUC_{0-24} by number of doses and dose level.

RESULTS

PopPK modeling

A total 64 neonates with a median (range) gestational age at birth of 39 weeks (35–42) and PNA and weight at the time of PK sampling of 7 days (3–30) and 3.2 kg (2.2–4.3), respectively, contributed 290 methylprednisolone plasma concentrations (**Figure S1**). Median number of samples per neonate was five (four to five). Median plasma concentration of methylprednisolone was 849 ng/mL (range 1.07–12,700); no samples were below the limit of quantification. A single dose of methylprednisolone of 30 mg/kg at the start of CPB was administered to 29 neonates (45%), whereas 35 (55%) received an additional dose approximately 10 hours before CPB (**Table 1**). A two-compartment model with first-order formation rate to methylprednisolone and estimation of the allometric coefficient on CL was selected as the base popPK model (**Figure S2**). No obvious trends were observed in the standard goodness-of-fit plots of the base model.

Table 1 Clinical data of subjects included in the analysis, N = 64

Characteristic	Infants, N = 64
Gestational age at birth, weeks	39 (34.6–42)
Postnatal age at 1st sample, days	7 (3–30)
Postmenstrual age at 1st sample, weeks	40 (36–44)
Body weight at 1st sample, kg	3.2 (2.2–4.3)
Serum creatinine at 1st sample, mg/dL	0.5 (0.1–1)
Cardiopulmonary bypass time, minutes	156.5 (64–251)
Lowest cardiopulmonary bypass flow rate, L/hour	0.1 (0–0.54)
Cross clamp time, minutes	71 (0–132)
Deep hypothermic circulatory arrest time, minutes	4.5 (0–42)
Time at low flow, minutes	30 (4–119)
Plasma lactate at 1st sample, mmol/L	1.8 (0.5–4.1)
Inotrope score	11.3 (2.5–20)
RACHS-1	
< 4	42%
≥4	58%
Female sex	47%
Race	
White	58%
Black	25%
Asian	2%
Latino	13%
Latino/black	2%
Latino/white	2%

Data were represented as median (range) for continuous data and % for categorical data. Where applicable, data were at the time of first dose. RACHS-1, Risk Adjustment for Congenital Heart Surgery.

After covariate selection (Figure S3 and Table S1), the final popPK model included CPB time as a covariate on CL: $CL = (3.88 \times (1 - \text{time after CPB (POSTCPB)}) + 3.88 \times \text{POSTCPB} \times (\text{CPBtime}/156.5)^{-0.47}) \times (\text{weight (WT)}/3.2)^{1.24}$

Table 2 Population PK parameters

Parameter	Estimate	RSE, %	Shrinkage, %	Bootstrap CI		
				2.5%	Median	97.5%
Structural PK model						
CL/F (L/hour, 3.2 kg)	3.88	8		3.32	3.90	4.57
Vc/F (L, 3.2 kg)	8.92	9		7.25	8.87	10.41
Q/F (L/hour, 3.2 kg)	0.10	24		0.045	0.096	0.13
Vp/F (L, 3.2 kg)	16.81	51		3.14	16.51	19.97
Kf (1/hour)	0.41	9		0.35	0.41	0.46
WT exponent on CL and Q	1.24	46		0.01	1.34	2.35
CPB time on CL	-0.47	47		-0.86	-0.46	0.079
IIV, %CV						
IIV, CL	47.2	31	4	32.6	45.7	59.8
IIV, Vc	26.4	90	45	0.3	24.3	43.9
IIV, Q	32.6	66	39	0.3	31.0	48.2
Residual variability						
Proportional error, %	42.8	17	14	35.1	42.5	50.4

$CL = (3.88 \times (1 - \text{POSTCPB}) + 3.88 \times \text{POSTCPB} \times (\text{CPB time}/156.5)^{-0.47}) \times (\text{WT}/3.2)^{1.24}$

CI, confidence interval; CL, clearance; CL/F, apparent clearance; CPB, cardiopulmonary bypass; %CV, coefficient of variance; IIV, interindividual variability; Kf, formation rate constant of methylprednisolone from methylprednisolone sodium succinate; PK, pharmacokinetic; POSTCPB, time after CPB; Q, distribution clearance; Q/F, apparent distribution clearance; RSE, relative standard error; Vc, volume of distribution of central compartment; Vc/F, apparent volume of distribution for central compartment; Vp/F, apparent volume of distribution for peripheral compartment; WT, weight.

(see control stream **Data S1**). The final estimated allometric coefficients were 1.24 for CL and Q. We repeated the covariate selection process after fixing allometric coefficients for WT at 0.75 and 1 for all CL and V parameters, respectively, and arrived at the same covariate model, although with slightly higher OFV and worse RSE on V_p when compared with the model with estimated allometric coefficients (OFV + 1.7 and RSE of V_p 96% vs. 51% for the model with fixed vs. estimated allometric coefficients).

Diagnostic plots for the final popPK model did not show obvious bias (Figure S4). Parameter estimates and their precision derived from the final popPK model are shown in Table 2. Median (range) *post hoc* empirical Bayesian estimates of CL pre-CPB and post-CPB were 1.28 L/hour/kg (0.25–2.71) and 1.24 L/hour/kg (0.20–3.60), respectively. Of the bootstrap data sets, 72% converged to > 3 significant digits. The medians of the bootstrap fixed effects parameter estimates were within 10% of the population estimates from the original data set for all parameters. The prediction-corrected visual predictive checks revealed a reasonable fit between the observed and predicted methylprednisolone concentrations (Figure S5), with 11% of the observed concentrations outside the 90% prediction interval.

PopPK/PD modeling

A total of 314 IL-6 data points from 62 neonates and 324 IL-10 data points from 64 neonates were used for popPK/PD modeling. The median (range) number of IL-6 and IL-10 data points per neonate was 6 (4–6). The median IL-6 and IL-10 concentrations during the study were 47.5 pg/mL (0–681.2) and 6.9 pg/mL (0.1–1125), respectively. The median IL-6 and IL-10 baseline concentrations were 9.5 pg/mL (0.7–83.3) and 1.3 pg/mL (0.1–9.5), respectively.

CPB effects on both IL-6 and IL-10 concentrations were best characterized by a separate CPB effect on R_{in} in parallel

with the methylprednisolone effect. Compared with a direct effect model, the OFV of an indirect effect model was lower for IL-6 (change in objective function value (Δ OFV) < -100) and IL-10 (Δ OFV < -120). For IL-6, the indirect response model with partial interaction between CPB effect and drug effect provided the best fit to the data and was selected as the base model (Figure S6). For IL-10, the indirect response model with complete interaction between CPB effect and drug effect provided the best fit to the data and was selected as the base model (Figure S7).

After covariate selection (Table S2, Figure S8, Table S3, Figure S9), the final IL-6 model included RACHS-1 on CPBE: $CPBE = 48.6 \times (2.59)^{RACHS-1 \geq 4}$ (Data S2). The final IL-10 model included postmenstrual age (PMA) on CPBE: $CPBE = 45.7 \times (PMA/40)^{14.8}$ (Data S3). Diagnostic plots for the final IL-6 and IL-10 popPK/PD models showed no obvious bias for IL-6 and a slight underprediction for IL-10 at high concentrations (Figures S10 and S11). Population PD parameters, covariate effects, and variability along with the standard error of these estimates and bootstrap output are shown in Tables 3 and 4.

The final model was evaluated using 500-set bootstrap analysis. The percent of bootstrap converging to > 3 significant digits was 81% and 77% for IL-6 and IL-10, respectively. The median of the bootstrap fixed effects parameter estimates were within 18% of the original population estimates for all parameters. The SVPCs revealed a reasonable fit between the observed and predicted IL-6 and IL-10 concentrations: 3.5% of observed average IL-6 responses fell outside the 90% prediction interval; 6.5% of observed average IL-10 responses fell outside the 90% prediction interval (Figures S12 and S13). Individual observed vs. simulation IL-6 and IL-10 concentrations are shown in Figure S14.

Simulations

No significant differences in simulated concentration time profiles of IL-6 and IL-10 were observed between 30 mg/kg and 10 mg/kg dose groups (Figures 1 and 2). Simulated IL-6 and IL-10 concentrations overall were > 50% lower and > 100% higher, respectively, following methylprednisolone administration when compared with placebo. Simulated IL-6 AUC_{0-24} was minimally lower following two doses of methylprednisolone when compared with a single dose (median AUC_{0-24} 2042.5 ng \times hour/mL vs. 2147 ng \times hour/mL, $P < 0.01$), and following 30 mg/kg compared with 10 mg/kg (1342 ng \times hour/mL vs. 1489 ng \times hour/mL, $P < 0.01$), but significantly lower when compared with placebo (4794 ng \times hour/mL, $P < 0.01$ when compared with all methylprednisolone dosing regimens). The magnitude of difference is shown in terms of AUC_{0-24} ratios in Table 5 and Table S4. Similarly, simulated IL-10 AUC was higher following any administration of methylprednisolone when compared with placebo (median IL-10 AUC_{0-24} following placebo 347 ng \times hour/mL, $P < 0.01$ when compared with all methylprednisolone dosing regimens), but did not differ significantly between any of the methylprednisolone dosing scenarios simulated (Table 5 and Table S5). Similar results were observed when simulations were stratified by patient and operative characteristics including PMA, RACHS-1 score, and CPB time: Methylprednisolone administration reduced IL-6 AUC_{0-24} and increased IL-10 AUC_{0-24} when compared with placebo without clinically significant differences between any of the dosing regimens simulated (Tables S4 and S5).

DISCUSSION

We developed the first popPK/PD model of methylprednisolone in neonates undergoing CPB and leveraged our

Table 3 Population PD parameters for IL-6

Parameter	Estimate	RSE, %	Shrinkage, %	Bootstrap CI		
				2.5%	Median	97.5%
Structural PK model						
I_{max}	1 FIX	NA		NA	NA	NA
IC_{50} , ng/mL	14	48		0.48	13.0	25.7
IL-6 _{base} , pg/mL	7.9	21		5.4	8.2	12.8
R_{out} , 1/hour	0.171	12		0.125	0.172	0.222
HILL	2.53	62		1.02	2.36	46.3
CPBE	48.6	61		20.6	57.4	857.2
Percent of CPB effect not interacting with MP, %	21.4	46		1.26	18.4	36.8
CPB effect half-life, hour	9.08	18		6.09	9.02	14.1
RACHS-1 ≥ 4 on CPBE	2.59	30		1.56	2.60	4.75
Interindividual variability, %CV						
IIV, IL-6 _{base}	100.5	33	11	58.7	97.3	124.5
IIV, CPBE	83.6	34	20	39.8	76.9	100.1
Residual variability						
Proportional error, %	54.1	10	9	49.0	54.4	59.5

CI, confidence interval; CPB, cardiopulmonary bypass; CPBE, fold change in IL-6 as a response to CPB procedure; %CV, coefficient of variance; HILL, Hill coefficient; IC_{50} , methylprednisolone concentration that produces 50% of maximum attainable inhibition; IIV, interindividual variability; IL-6, interleukin-6 plasma concentration; IL-6_{base}, model predicted IL-6 plasma concentration in subjects prior to the first dose of methylprednisolone; I_{max} , maximum fold change in production of IL-6 as a response to drug exposure; R_{out} , first-order rate constant for decline of IL-6; MP, methylprednisolone; PD, pharmacodynamics; PK, pharmacokinetics; RACHS-1, Risk Adjustment for Congenital Heart Surgery; RSE, relative standard error.

Table 4 Population PD parameters for IL-10

Parameter	Estimate	RSE, %	Shrinkage, %	Bootstrap CI		
				2.5%	Median	97.5%
Structural PK model						
S_{max}	2.28	24		1.34	2.44	4.41
SC_{50} , ng/mL	58.2	52		22.5	68.3	176.8
IL-10 _{base} , pg/mL	1.52	12		1.25	1.54	1.91
R_{out} , 1/hour	0.542	12		0.43	0.55	0.66
HILL	3.58	90		1.12	3.65	9.09
CPBE	45.7	16		30.9	44.7	63.5
PMA on CPBE	14.8	29		6.76	15.2	26.7
IIV, %CV						
IIV, S_{max}	110	33	20	62.9	106	141
IIV, IL-10 _{base}	64.7	23	11	46.2	63.0	77.6
IIV, CPBE	88.1	32	16	50.9	81.2	111
Residual variability						
Proportional error, %	53.8	9	15	48.2	53.5	58.3

CI, confidence interval; CPBE, fold change in IL-6 as a response to CPB procedure; %CV, coefficient of variance; IIV, interindividual variability; IL-10, interleukin-10 plasma concentration; IL-10_{base}, model predicted IL-10 plasma concentration in subjects prior to the first dose of methylprednisolone; R_{out} , first-order rate constant for decline of IL-6; PD, pharmacodynamics; PK, pharmacokinetics; PMA, postmenstrual age; RACHS-1, Risk Adjustment for Congenital Heart Surgery; RSE, relative standard error; S_{max} , maximum fold change in production of IL-10 as a response to drug exposure; SC_{50} , methylprednisolone concentration that produces 50% of maximum attainable stimulation; HILL, Hill coefficient.

model to perform dosing simulations for methylprednisolone in this population. The PK of methylprednisolone has been previously characterized using one-compartment models in both healthy adults and those undergoing CPB.^{23,27} A two-compartment model better characterized the data in our study. This may be related to the lower limit of quantification of our methylprednisolone assay (1 ng/mL) compared with those used in previous studies (5, 10, 25, 50 ng/mL), which allowed our model to better characterize the terminal elimination phase of methylprednisolone without being hampered by below-quantification limit values. We estimated typical values of the apparent clearance (CL/F) and apparent volume of distribution at steady state (V_{ss}/F as a sum of apparent volume of distribution for central compartment and apparent volume of distribution for peripheral compartment) for an average neonate with a body weight of 3.2 kg at 3.8 L/hour and 26.3 L, respectively.

To our knowledge, PK parameters of methylprednisolone have never been reported in neonates or infants. However, CL/F and apparent volume of distribution after non-i.v. administration of methylprednisolone after i.v. administration of methylprednisolone hemisuccinate in children with inflammatory bowel disease (mean [standard deviation] age: 11.3 [2.5] years) were 0.98 L/hour/kg and 1.53 L/kg, respectively.²⁸ Although our estimates of CL/F were only slightly higher (1.18 L/hour/kg), our estimate of V_{ss}/F (8.2 L/kg) was about fivefold greater. This may be related to CPB effects, including inflammation and capillary leak, adsorption of drug by the CPB circuit, increased volume of distribution from the circuit tubing, and hypoalbuminemia with a secondary increase in free drug concentration.²⁹ In addition, the formation of methylprednisolone from its prodrug in adults undergoing CPB has been shown to be reduced by decreased liver perfusion and reduced metabolic activity

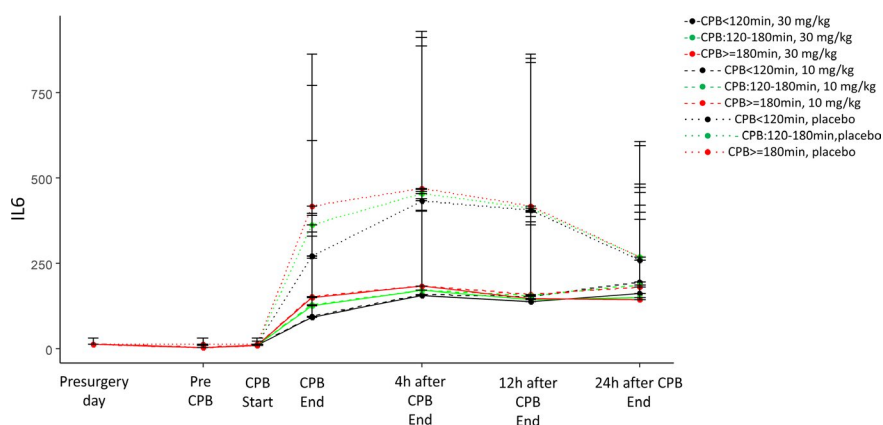


Figure 1 Simulated IL-6 concentrations. Simulated IL-6 plasma concentrations (pg/mL) following different dosing regimens. CPB, cardiopulmonary bypass; h, hour; IL-6, interleukin-6; min, minute.

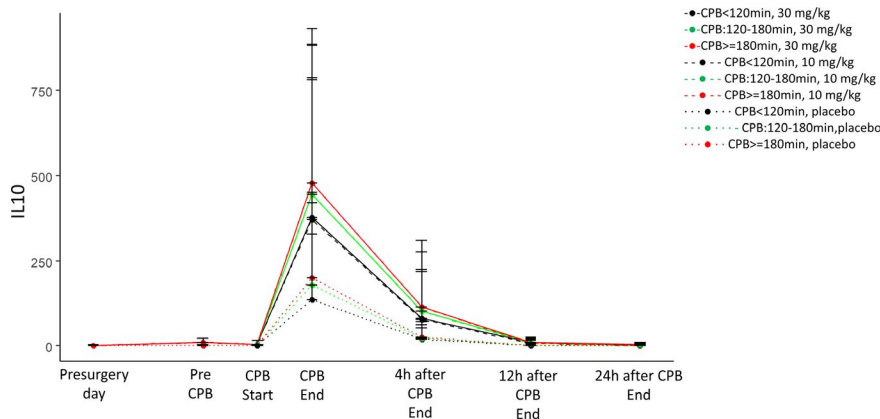


Figure 2 Simulated IL-10 concentrations. Simulated IL-10 plasma concentrations (pg/mL) following different dosing regimens. CPB, cardiopulmonary bypass; h, hour; IL-10, interleukin-10; min, minute.

Table 5 Mean (95% CI) ratios of simulated AUC from time 0 to 24 hours after CPB start (AUC_{0-24}) of IL-6 and IL-10 following different dose regimens of methylprednisolone and placebo

Ratio	IL-6	IL-10
2 vs. 1 dose of methylprednisolone	0.92 (0.92–0.95)	1.08 (1.08–1.10)
30 vs. 10 mg/kg of methylprednisolone	0.89 (0.89–0.89)	1.03 (1.03–1.04)
10 mg/kg of methylprednisolone vs. placebo	0.27 (0.27–0.27)	3.85 (3.79–3.90)

AUC, area under the concentration-time curve; AUC_{0-24} , area under the concentration time curve from time 0 to 24 hours; CI, confidence interval; CPB, cardiopulmonary bypass; IL-6, interleukin-6; IL-10, interleukin-10.

during CPB.²³ In our study, the estimated formation rate of methylprednisolone in infants on CPB was even lower when compared with adults on CPB (0.4 1/hour vs. 0.7 1/hour).²³ Therefore, the greater value of CL/F and V_{ss}/F of methylprednisolone in infants undergoing CPB may be explained by the decreased formation of methylprednisolone from the prodrug during CPB.

Direct and indirect effect PD models have been used to characterize the time course of inflammatory cell counts after methylprednisolone.^{30,31} This is the first PD model characterizing the methylprednisolone effect on cytokines in patients undergoing CPB. The indirect effect models characterized the plasma concentration time profiles of IL-6 and IL-10 better than direct effect models. This is consistent with the drug's mechanism of action: Methylprednisolone reduces complement-mediated activation of neutrophils and inhibits the secretion of proinflammatory cytokines, including IL-6.^{32–34} A previous study suggested the increase in anti-inflammatory cytokine IL-10 may be a part of compensation for increased proinflammatory cytokines.³⁵ Both effects can be assumed to be delayed relative to the time of plasma exposure. The methylprednisolone concentration that produces 50% of maximum attainable stimulation (SC_{50}) was estimated to be 58 ng/mL for the methylprednisolone effect on IL-10, and IC_{50} was estimated to be 14 ng/mL for the methylprednisolone effect on IL-6. To our knowledge, the SC_{50} for the methylprednisolone effect on cytokines has not been reported. However, the SC_{50} and

IC_{50} for the methylprednisolone effect on blood histamine concentrations estimated using different PD models ranged from 2.73 ng/mL²² to 113 ng/mL.³⁶ Our values fall within this, albeit wide, range.

CPB time was a significant covariate on CL and longer CPB time was associated with lower methylprednisolone CL. Methylprednisolone is primarily metabolized in the liver with < 10% excreted unchanged in urine, so the relationship between CPB time and CL may be explained by decreased liver blood flow and metabolic activity as a result of hypothermia during CPB.³⁷ In infants, these changes may be enhanced because of a greater decrease in body temperature relative to adults, lower bypass flow rates, and the occasional use of complete circulatory arrest or regional cerebral perfusion (i.e., period of no blood flow to organs other than the brain), which are infrequently employed in adults.³⁸

RACHS-1 was identified as a significant covariate for the CPB effect on IL-6. RACHS-1 is a predictor of mortality in patients undergoing congenital heart surgery.^{39,40} A higher score is indicative of higher surgical complexity and associated with greater disease severity and longer CPB time. The model predicted greater increase in IL-6 concentration due to CPB in patients with higher RACHS-1, which may be related to the longer CPB time required for surgery. For IL-10, PMA was identified as a significant covariate on the CPB effect. When comparing the most premature infant included in our cohort (34 weeks gestational age) to a full-term infant (40 weeks gestational age), the CPB effect on IL-10 production was ~ 10-fold higher in the full-term infant when compared with the preterm infant. A positive monotone trend in the expression of genes involved in immune system development in preterm neonates has been reported.⁴¹ The greater magnitude of CPB effect in older infants may be explained by the maturation of the immune system in the early life stage. Because our model-building steps were primarily guided by statistical considerations, PMA was not included as a covariate in the IL-6 model. Although we can only speculate as to the biological reasons behind the observed statistical difference, the critical role played by anti-inflammatory IL-10 in the maintenance of a state of relative immune tolerance between the fetus and the maternal organism prior to delivery may explain why it is more readily

affected by early maturational changes. Conversely, IL-6 has shown rather robust expression in neonates, reaching or even exceeding adult levels.⁴²

Our simulation results suggest that both 10 mg/kg and 30 mg/kg of methylprednisolone produced significant anti-inflammatory effect (as measured by the IL-6 and IL-10 concentrations) when compared with placebo. No substantial difference in the effect of methylprednisolone on IL-6 and IL-10 was observed between 10 mg/kg dose and 30 mg/kg doses. This suggests that a 30 mg/kg dose is unlikely to provide significant additional benefit when compared with 10 mg/kg. This finding is consistent with prior reports of clinical end points, including intensive care unit length of stay, hospital length of stay, and the occurrence of low cardiac output syndrome.^{16,17} No substantial difference in the effect of methylprednisolone on IL-6 and IL-10 concentrations was observed following one-dose vs. two-dose regimens. This finding suggests that an additional methylprednisolone dose given on the day prior to surgery may not be necessary. Again, this is consistent with previously reported clinical assessments, including inotropic requirement, duration of postoperative mechanical ventilation, and intensive care unit and hospital length of stay.²²

Limitations of our study include the relatively sparse PD data collected after methylprednisolone administration and prior to and during CPB and the single-dose level administered to all infants. We further assumed that all dosing, including dose administered into the CPB circuit, are essentially administered into a depot compartment from which the prodrug methylprednisolone sodium succinate is entirely converted into methylprednisolone. This differs from the previously published adult PK model, where methylprednisolone sodium succinate was modeled to undergo both conversion to methylprednisolone and renal CL.²³ A future study with richer PD sampling after methylprednisolone administration and prior to CPB, PD measurements collected during CPB, longer sampling time after CPB (especially for IL-6), additional dosing levels of methylprednisolone, and differentiation between prodrug and methylprednisolone concentrations in plasma and urine may help better characterize the PD of methylprednisolone. Sampling during CPB in particular may uncover significant changes in anti-inflammatory effect resulting from altered methylprednisolone exposure, as previously shown for other drugs.^{43,44} Richer sampling may also allow for the identification of additional covariate effects beyond those included in our model and may help better characterize the concentration-time profile differences between IL-6, IL-10, and other inflammatory biomarkers. Importantly, although both IL-6 and IL-10 are known to be implicated in the inflammatory cascade induced by CPB in infants and have been previously studied in this population, other biomarkers may be better suited to characterize methylprednisolone's effect. Finally, although it is reasonable to postulate that modulating inflammatory response would lead to improved clinical outcomes, it is important to point out that a clear relationship between methylprednisolone administration and clinical end points has not yet been established.⁴⁵ This

may be partially a result of the fact that optimal levels of inflammatory biomarkers are unknown, limiting our ability to identify dose-response relationships and optimal dosing of methylprednisolone and other anti-inflammatory drugs. A large, multicenter, randomized controlled trial is currently underway to assess the drug's effect on a clinical composite end point of cardiovascular outcomes.⁴⁶ Finally, we estimated allometric coefficients for WT in our final model, which may limit comparability to models with fixed allometric coefficients and may preclude the scaling of our estimated PK parameters to a non-neonatal population. Standardizing approaches to reporting PK parameters in pediatric studies by combining fixed allometric exponents with a maturation function and standardizing CL and *V* parameters to 70 kg adult body weight may be preferable.⁴⁷ The theory-based allometric exponents will account for changes related to size, whereas the sigmoidal PMA function illustrates the maturation of CL processes, which is essential when the study population includes children younger than the age of 2 years. Nevertheless, maintaining fixed allometric coefficients at 0.75 for CL and 1 for *V* parameters in a neonatal or infant population without the inclusion of a function illustrating the effect of age and maturation would not provide a physiological representation of the relationship between weight and organ function in this age range.⁴⁸ Estimating the allometric coefficient provides an alternative, although less desirable than the inclusion of a maturation function, to represent the combined effects of growth and maturation. Given our inability to identify a maturation function as a covariate on CL, likely because of the overall sparsity of available PK data, we resorted to this alternative. Yet reassuringly, our estimated allometric exponent of 1.24 is consistent with previously published analyses that have shown that an allometric exponent of 1.2 is optimal when predicting drug CL in children ≤ 3 months of age without the inclusion of a separate maturation function.⁴⁹ Nonetheless, it is important to highlight that based on the sample size of our study and the observed between-subject variability in CL, this estimated allometric coefficient is likely biased by our population; the extrapolation of CL estimates to older children or other populations may not be readily feasible.⁵⁰ Given the objectives of our study and the fact that methylprednisolone is not routinely administered on CPB outside of the neonatal period, this limitation may be acceptable.

In conclusion, we found that indirect-response PK/PD models characterized the effects of methylprednisolone administration on proinflammatory and anti-inflammatory cytokines in infants undergoing surgery on CPB. Simulations suggested no additional benefit from dosing > 10 mg/kg, or multiple dosing, but significantly improved cytokine profile when compared with placebo. Our model, the first of its kind in this patient population, has implications for the design of future clinical trials in this population.

Supporting Information. Supplementary information accompanies this paper on the *CPT: Pharmacometrics & Systems Pharmacology* website (www.psp-journal.com).

Methods. Supplementary Methods

Figure S1. Observed concentration-time plots: Methylprednisolone concentration vs. time after last dose with concentration on log scale (A), methylprednisolone concentration vs. time after last dose with concentration on linear scale (B), methylprednisolone concentration vs. time after first dose with concentration on log scale (C), and methylprednisolone concentration vs. time after first dose with concentration on linear scale (D).

Figure S2. Base population PK model diagnostic plots: observed vs. individual prediction (A) and population prediction (B), conditional weighted residuals vs. population predictions (C), and time after last dose (D). PK, pharmacokinetics.

Figure S3. ETA for clearance (ETA_{CL}) vs. postmenstrual age (PMA) (A), postnatal age (PNA) (B), crossclamp time (C), and CPB time (D) (each closed circle represents a patient) for the base PK model. CPB, cardiopulmonary bypass; PK, pharmacokinetics.

Figure S4. Final population PK model diagnostic plots: observed vs. individual prediction (A) and population prediction (B), conditional weighted residuals vs. population predictions (C), and time after last dose (D). PK, pharmacokinetics.

Figure S5. Prediction-corrected visual predictive check of methylprednisolone.

Figure S6. Base population PD model for IL-6 diagnostic plots: observed vs. individual prediction (A) and population prediction (B), conditional weighted residuals vs. population predictions (C), and time after last dose (D). IL-6, interleukin-6 plasma concentration; PD, pharmacodynamics.

Figure S7. Base population PD model for IL-10 diagnostic plots: observed vs. individual prediction (A) and population prediction (B), conditional weighted residuals vs. population predictions (C), and time after last dose (D). IL-10, interleukin-10 plasma concentration; PD, pharmacodynamics.

Figure S8. ETA for IL-6 Base (ETA_{Base}) vs. postmenstrual age (PMA) (A), gestational age (GA) (B), and ETA for CPBE (ETA_{CPBE}) vs. RACHS-1 (RANK) (C), and deep hypothermic circulatory arrest (D) (each closed circle represents a patient) for the base PD model for IL-6. CPBE, fold change in IL-6 as a response to CPB procedure; IL-6, interleukin-6 plasma concentration; PD, pharmacodynamics; RACHS-1, Risk Adjustment for Congenital Heart Surgery.

Figure S9. ETA for IL-10 Base (ETA_{Base}) vs. postnatal age (PNA) (A), gestational age (GA) (B), and ETA for CPBE (ETA_{CPBE}) vs. postmenstrual age (PMA) (each closed circle represents a patient) for the base PD model for IL-10. CPBE, fold change in IL-6 as a response to CPB procedure; IL-6, interleukin-6 plasma concentration; IL-10, interleukin-10 plasma concentration; PD, pharmacodynamics.

Figure S10. Final population PD model for IL-6 diagnostic plots: observed vs. individual prediction (A) and population prediction (B), conditional weighted residuals vs. population predictions (C), and time after last dose (D). IL-6, interleukin-6 plasma concentration; PD, pharmacodynamics.

Figure S11. Final population PD model for IL-10 diagnostic plots: observed vs. individual prediction (A) and population prediction (B), conditional weighted residuals vs. population predictions (C), and time after last dose (D). IL-10, interleukin-10 plasma concentration; PD, pharmacodynamics.

Figure S12. Standardized visual predictive check of IL-6 observation percentiles vs. time after last dose (A) and observation percentiles vs. time point (B). Open circles represent calculated percentiles. IL-6, interleukin-6 plasma concentration.

Figure S13. Standardized visual predictive check of IL-10 observation percentiles vs. time after last dose (A) and observation percentiles vs.

time point (B). Open circles represent calculated percentiles. IL-10, interleukin-10 plasma concentration.

Figure S14. Plots of individual observed vs. predicted IL-6 (pg/mL) vs time after first dose (A and B) and plots of individual observed vs. predicted IL-10 plasma concentrations (pg/mL) vs. time after first dose (C and D). IL-6, interleukin-6 plasma concentration; IL-10, interleukin-10 plasma concentration.

Table S1. Summary of the population PK model building steps. PK, pharmacokinetics.

Table S2. Summary of the model building steps for IL-6. IL-6, interleukin-6 plasma concentration.

Table S3. Summary of the model building steps for IL-10. IL-10, interleukin-10 plasma concentration.

Table S4. Summary of AUC₀₋₂₄ for IL-6 in all groups. AUC₀₋₂₄, area under the concentration time curve from time 0 to 24 hours; IL-6, interleukin-6 plasma concentration.

Table S5. Summary of AUC₀₋₂₄ for IL-10 in all groups. AUC₀₋₂₄, area under the concentration time curve from time 0 to 24 hours; IL-10, interleukin-10 plasma concentration.

Data S1.

Data S2.

Data S3.

Acknowledgments. C.H. receives salary support from the Eunice Kennedy Shriver National Institute of Child Health and Human Development (NICHD, K23HD090239) and industry for drug development in children. D.G. receives support for research from the Eunice Kennedy Shriver National Institute of Child Health and Human Development (NICHD, 5K23HD083465 and 1R01HD096435). K.H. and E.G. receive support from the National Centers for Advancing Translational Sciences for their work related to methylprednisolone effects on post-operative outcomes after congenital heart surgery (U01TR-001803-01). M.C.W. receives support for research from the National Institutes of Health (R01-HD076676), National Institute of Allergy and Infectious Diseases (HHSN2722015000061 and HHSN2722013000171), NICHD (HHSN2752010000031), the Biomedical Advanced Research and Development Authority (HHSO100201300009C), and industry for drug development in adults and children.

Funding. This study was funded by the Eunice Kennedy Shriver National Institute of Child Health and Human Development (NICHD) award 1K23HD090239 (principal investigator, Hornik).

Conflict of Interest. E.G. is a research consultant for Bayer. All other authors declared no competing interests for this work.

Author Contributions. C.P.H. wrote the paper. C.P.H., D.G., J.D., E.G., K.D.H., and M.C.W. designed the research. C.P.H. and E.G. performed the research. C.P.H., D.G., and H.W. analyzed the data.

1. Petrini, J., Damus, K., Russell, R., Poschman, K., Davidoff, M.J. & Mattison, D. Contribution of birth defects to infant mortality in the United States. *Teratology* **66**(suppl. 1), S3-S6 (2002).
2. Yang, Q., Chen, H., Correa, A., Devine, O., Mathews, T.J. & Honein, M.A. Racial differences in infant mortality attributable to birth defects in the United States, 1989-2002. *Birth Defects Res. A. Clin. Mol. Teratol.* **76**, 706-713 (2006).
3. Dönmez, A. & Yurdakök, O. Cardiopulmonary bypass in infants. *J. Cardiothorac. Vasc. Anesth.* **28**, 778-788 (2014).
4. Kolackova, M. et al. The effect of conventional and mini-invasive cardiopulmonary bypass on neutrophil activation in patients undergoing coronary artery bypass grafting. *Mediators Inflamm.* **2012**, 152895 (2012).
5. Kagawa, H. et al. Inflammatory response to hyperoxemic and normoxemic cardiopulmonary bypass in acyanotic pediatric patients. *World J. Pediatr. Congenit. Heart. Surg.* **5**, 541-545 (2014).

6. Chew, M.S. *et al.* Tissue injury and the inflammatory response to pediatric cardiac surgery with cardiopulmonary bypass: a descriptive study. *Anesthesiology* **94**, 745–753, discussion 5A (2001).
7. Butler, J. *et al.* Acute-phase responses to cardiopulmonary bypass in children weighing less than 10 kilograms. *Ann. Thorac. Surg.* **62**, 538–542 (1996).
8. Pasquali, S.K. *et al.* Perioperative methylprednisolone and outcome in neonates undergoing heart surgery. *Pediatrics* **129**, e385–e391 (2012).
9. Ito, S., Kusunoki, Y., Oka, T., Ito, Y., Okuno, A. & Yoshioka, H. Pharmacokinetics of high-dose methylprednisolone in children. *Dev. Pharmacol. Ther.* **19**, 99–105 (1992).
10. Kong, A.N. & Jusko, W.J. Disposition of methylprednisolone and its sodium succinate prodrug in vivo and in perfused liver of rats: nonlinear and sequential first-pass elimination. *J. Pharm. Sci.* **80**, 409–415 (1991).
11. Czock, D., Keller, F., Rasche, F.M. & Häussler, U. Pharmacokinetics and pharmacodynamics of systemically administered glucocorticoids. *Clin. Pharmacokinet.* **44**, 61–98 (2005).
12. Nollert, G., Sperling, J., Sakamoto, T., Jaeger, B.R. & Jonas, R.A. Higher hematocrit improves liver blood flow and metabolism during cardiopulmonary bypass in piglets. *Thorac. Cardiovasc. Surg.* **49**, 226–230 (2001).
13. O'Rullian, J.J., Wise, R.K., McCoach, R.M., Kingsley, C.P. & Williams, D.R. The effects of haemofiltration on cefazolin levels during cardiopulmonary bypass. *Perfusion* **13**, 176–180 (1998).
14. Wood, M., Shand, D.G. & Wood, A.J. Propranolol binding in plasma during cardiopulmonary bypass. *Anesthesiology* **51**, 512–516 (1979).
15. van Saet, A., de Wildt, S.N., Knibbe, C.A., Bogers, A.D., Stolker, R.J. & Tibboel, D. The effect of adult and pediatric cardiopulmonary bypass on pharmacokinetic and pharmacodynamic parameters. *Curr. Clin. Pharmacol.* **8**, 297–318 (2013).
16. Graham, E.M. *et al.* Preoperative steroid treatment does not improve markers of inflammation after cardiac surgery in neonates: results from a randomized trial. *J. Thorac. Cardiovasc. Surg.* **147**, 902–908 (2014).
17. Keski-Nisula, J. *et al.* Methylprednisolone in neonatal cardiac surgery: reduced inflammation without improved clinical outcome. *Ann. Thorac. Surg.* **95**, 2126–2132 (2013).
18. Liakopoulos, O.J. *et al.* Cardiopulmonary and systemic effects of methylprednisolone in patients undergoing cardiac surgery. *Ann. Thorac. Surg.* **84**, 110–118, discussion 118–119 (2007).
19. McBride, W.T. *et al.* Methylprednisolone favourably alters plasma and urinary cytokine homeostasis and subclinical renal injury at cardiac surgery. *Cytokine* **27**, 81–89 (2004).
20. Schroeder, V.A., Pearl, J.M., Schwartz, S.M., Shanley, T.P., Manning, P.B. & Nelson, D.P. Combined steroid treatment for congenital heart surgery improves oxygen delivery and reduces postbypass inflammatory mediator expression. *Circulation* **107**, 2823–2828 (2003).
21. Kong, A.N. *et al.* Pharmacokinetics and pharmacodynamic modeling of direct suppression effects of methylprednisolone on serum cortisol and blood histamine in human subjects. *Clin. Pharmacol. Ther.* **46**, 616–628 (1989).
22. Graham, E.M. *et al.* Standardized preoperative corticosteroid treatment in neonates undergoing cardiac surgery: results from a randomized trial. *J. Thorac. Cardiovasc. Surg.* **142**, 1523–1529 (2011).
23. Kong, A.N., Jungbluth, G.L., Pasko, M.T., Beam, T.R. & Jusko, W.J. Pharmacokinetics of methylprednisolone sodium succinate and methylprednisolone in patients undergoing cardiopulmonary bypass. *Pharmacotherapy* **10**, 29–34 (1990).
24. Bergstrand, M., Hooker, A.C., Wallin, J.E. & Karlsson, M.O. Prediction-corrected visual predictive checks for diagnosing nonlinear mixed-effects models. *AAPS. J.* **13**, 143–151 (2011).
25. Wang, D.D. & Zhang, S. Standardized visual predictive check versus visual predictive check for model evaluation. *J. Clin. Pharmacol.* **52**, 39–54 (2012).
26. Al-Radi, O.O. *et al.* Case complexity scores in congenital heart surgery: a comparative study of the Aristotle Basic Complexity score and the Risk Adjustment in Congenital Heart Surgery (RACHS-1) system. *J. Thorac. Cardiovasc. Surg.* **133**, 865–875 (2007).
27. Lew, K.H. *et al.* Gender-based effects on methylprednisolone pharmacokinetics and pharmacodynamics. *Clin. Pharmacol. Ther.* **54**, 402–414 (1993).
28. Faure, C. *et al.* Pharmacokinetics of intravenous methylprednisolone and oral prednisone in paediatric patients with inflammatory bowel disease during the acute phase and in remission. *Eur. J. Clin. Pharmacol.* **54**, 555–560 (1998).
29. Sinclair, D.G., Haslam, P.L., Quinlan, G.J., Pepper, J.R. & Evans, T.W. The effect of cardiopulmonary bypass on intestinal and pulmonary endothelial permeability. *Chest* **108**, 718–724 (1995).
30. Hon, Y.Y., Jusko, W.J., Sprattlin, V.E. & Jann, M.W. Altered methylprednisolone pharmacodynamics in healthy subjects with histamine N-methyltransferase C314T genetic polymorphism. *J. Clin. Pharmacol.* **46**, 408–417 (2006).
31. Lee, S.J. *et al.* Reduced methylprednisolone clearance causing prolonged pharmacodynamics in a healthy subject was not associated with CYP3A5*3 allele or a change in diet composition. *J. Clin. Pharmacol.* **46**, 515–526 (2006).
32. Bourbon, A. *et al.* The effect of methylprednisolone treatment on the cardiopulmonary bypass-induced systemic inflammatory response. *Eur. J. Cardiothorac. Surg.* **26**, 932–938 (2004).
33. Tenenbergs, S.D., Bailey, W.W., Cotta, L.A., Brodt, J.K. & Solomkin, J.S. The effects of methylprednisolone on complement-mediated neutrophil activation during cardiopulmonary bypass. *Surgery* **100**, 134–142 (1986).
34. Kawamura, T., Inada, K., Okada, H., Okada, K. & Wakusawa, R. Methylprednisolone inhibits increase of interleukin 8 and 6 during open heart surgery. *Can. J. Anaesth.* **42**, 399–403 (1995).
35. Kawamura, T., Inada, K., Nara, N., Wakusawa, R. & Endo, S. Influence of methylprednisolone on cytokine balance during cardiac surgery. *Crit. Care. Med.* **27**, 545–548 (1999).
36. Daley-Yates, P.T., Gregory, A.J. & Brooks, C.D. Pharmacokinetic and pharmacodynamic assessment of bioavailability for two prodrugs of methylprednisolone. *Br. J. Clin. Pharmacol.* **43**, 593–601 (1997).
37. Al-Habet, S.M. & Rogers, H.J. Methylprednisolone pharmacokinetics after intravenous and oral administration. *Br. J. Clin. Pharmacol.* **27**, 285–290 (1989).
38. Haessler, D., Reverdy, M.E., Neidecker, J., Brûlé, P., Ninet, J. & Lehot, J.J. Antibiotic prophylaxis with cefazolin and gentamicin in cardiac surgery for children less than ten kilograms. *J. Cardiothorac. Vasc. Anesth.* **17**, 221–225 (2003).
39. Jenkins, K.J. Risk adjustment for congenital heart surgery: the RACHS-1 method. *Semin. Thorac. Cardiovasc. Surg. Pediatr. Card. Surg. Annu.* **7**, 180–184 (2004).
40. Jacobs, J.P. *et al.* Stratification of complexity improves the utility and accuracy of outcomes analysis in a Multi-Institutional Congenital Heart Surgery Database: Application of the Risk Adjustment in Congenital Heart Surgery (RACHS-1) and Aristotle Systems in the Society of Thoracic Surgeons (STS) Congenital Heart Surgery Database. *Pediatr. Cardiol.* **30**, 1117–1130 (2009).
41. Zasada, M., Kwinta, P., Durlak, W., Bik-Multanowski, M., Madetko-Talowska, A. & Pietrzyk, J.J. Development and maturation of the immune system in preterm neonates: results from a whole genome expression study. *Biomed. Res. Int.* **2014**, 498318 (2014).
42. Kollmann, T.R., Levy, O., Montgomery, R.R. & Goriely, S. Innate immune function by Toll-like receptors: distinct responses in newborns and the elderly. *Immunity* **37**, 771–783 (2012).
43. Zuppa, A.F. *et al.* Population pharmacokinetics of milrinone in neonates with hypoplastic left heart syndrome undergoing stage I reconstruction. *Anesth. Analg.* **102**, 1062–1069 (2006).
44. Himebauch, A.S. *et al.* Skeletal muscle and plasma concentrations of cefazolin during cardiac surgery in infants. *J. Thorac. Cardiovasc. Surg.* **148**, 2634–2641 (2014).
45. Scrascia, G. *et al.* Perioperative steroids administration in pediatric cardiac surgery: a meta-analysis of randomized controlled trials*. *Pediatr. Crit. Care. Med.* **15**, 435–442 (2014).
46. Hill, K.D. & Kannankeril, P.J. Perioperative corticosteroids in children undergoing congenital heart surgery: five decades of clinical equipoise. *World. J. Pediatr. Congenit. Heart. Surg.* **9**, 294–296 (2018).
47. Holford, N. *et al.* A Pharmacokinetic standard for babies and adults. *J. Pharm. Sci.* **102**, 2941–2952 (2013).
48. Mahmood, I. Dosing in children: a critical review of the pharmacokinetic allometric scaling and modelling approaches in paediatric drug development and clinical settings. *Clin. Pharmacokinet.* **53**, 327–346 (2014).
49. Mahmood, I. Prediction of drug clearance in children 3 months and younger: an allometric approach. *Drug. Metabol. Drug. Interact.* **25**, 25–34 (2010).
50. Sinha, J. *et al.* Choosing the allometric exponent in covariate model building. *Clin. Pharmacokinet.* **58**, 89–100 (2019).

© 2019 The Authors. *CPT: Pharmacometrics & Systems Pharmacology* published by Wiley Periodicals, Inc. on behalf of the American Society for Clinical Pharmacology and Therapeutics. This is an open access article under the terms of the Creative Commons Attribution-NonCommercial License, which permits use, distribution and reproduction in any medium, provided the original work is properly cited and is not used for commercial purposes.